Effects of Molecular Weight Distribution on the Dynamics of the Early Stage of Spinodal Decomposition

Mikihito Takenaka and Takeji Hashimoto*

Division of Polymer Chemistry, Graduate School of Engineering, Kyoto University, Kyoto 606-01, Japan

Received May 23, 1994; Revised Manuscript Received July 15, 1994®

ABSTRACT: We studied the effects of the molecular weight distribution (MWD) on the dynamics of the early stage spinodal decomposition (SD) in poly(styrene-*ran*-butadiene) (SBR)/polybutadiene (PB) mixtures by using time-resolved light scattering techniques. In order to study the effects, we used four binary mixtures of SBR/PB with a given composition in which the PB components have the same weight-average molecular weight but different MWDs. The time changes in scattered intensity profiles of the four SBR/PB mixtures can be described by Cahn's linearized theory over the range of wavenumbers covered in this study. The characteristic parameters such as the collective diffusion coefficient and the characteristic wavenumber of which the scattered intensity increases with time at a maximum rate were analyzed on the basis of the linearized theory. The characteristic parameters for the four mixtures turned out to be identical so that the dynamics was found to be insensitive to MWD, depending on the weight-average molecular weight.

I. Introduction

The dynamics of phase separation via spinodal decomposition (SD) in binary polymer mixtures provides a fascinating research theme in nonequilibrium statistical physics.[1-8] Advantages of studying polymers may be linked to the following unique features: (i) the spatial scale of the concentration fluctuations developed is much larger and (ii) the dynamics is much slower than the counterparts in small-molecule mixtures. Features i and ii may facilitate a quantitative study of SD, and the results obtained may enrich our knowledge in nonequilibrium statistical mechanics. For example, the results obtained by experiments in binary polymer mixtures were compared with those obtained by computer simulations in detail and both results are found to be in quantitative agreement.[7-9] This result may provide new information on the dynamics of phase separation via SD.

Polymer mixtures, however, have features which do not exist in simple small-molecule mixtures. One of the features is the effects of molecular weight distribution (MWD) inherent in polymer systems. The MWD affects not only static behavior (e.g. the scattered intensity in the one-phase region,[10] the spinodal point, and the coexistence curve[11]) but also dynamical behavior. Despite the importance of its research, there are few theories and computer simulations[12,13] concerning the MWD effects on the dynamics of phase separation via SD. Here we present the initial results of our experiments for this problem.

One of the most interesting issues is whether the dynamics of the early stage SD can be approximated by the linearized theory. The linearized theory without the thermal noise effects was first derived for a metal alloy by Cahn.[14] Subsequently, Cook[15] introduced the thermal noise effects into the theory. de Gennes,[16] Pincus,[17] and Binder[18] applied the theory to polymer blends. In the early stage of SD of an A/B polymer blend with no molecular weight distribution, the time evolution of the structure factor ($S(q,t)$ for wavenumber q and at time t is described by the Cahn–Hilliard–Cook theory[18]

$$S(q,t) = S(q,\infty) + [S(q,0) - S(q,\infty)] \exp[2R(q)t] \quad (1)$$

where $S(q,0)$, $S(q,\infty)$, and $R(q)$ are the $S(q,t)$ at $t = 0$, the virtual structure factor, and the growth rate of the q Fourier mode of the fluctuations, respectively. For the small q region observed in our light scattering experiments, i.e., $qR_{g,A} \ll 1$ and $qR_{g,B} \ll 1$, $S(q,\infty)$ is given by

$$\frac{1}{S(q,\infty)} = \frac{1}{\phi_A N_A} + \frac{1}{\phi_B N_B} - 2\chi + \frac{1}{18}\left(\frac{a_A^2}{\phi_A} + \frac{a_B^2}{\phi_B}\right)q^2 \quad (2)$$

where ϕ_K is the volume faction of the K component (K = A or B) and N_K and a_K are, respectively, the polymerization index and the statistical segment length of K. χ is the Flory–Huggins segmental interaction parameter per segment between A and B at the phase separation temperature. For a large quench depth and at a sufficiently long time in the early stage of SD, the thermal noise effect is negligible and the time evolution of $S(q,t)$ at small q is expressed by Cahn's theory:[14]

$$S(q,t) = S(q,0) \exp[2R(q)t] \quad (3)$$

The growth rate $R(q)$ is given by

$$R(q) = -q^2\Lambda(0)\frac{1}{S(q,\infty)} \quad (4)$$

where $\Lambda(0)$ is the Onsager kinetic coefficient of the system in the small q limit. $\Lambda(0)$ is given by[18]

$$\frac{1}{\Lambda(0)} = \frac{1}{D_A N_A \phi_A} + \frac{1}{D_B N_B \phi_B} \quad (5)$$

for incompressible mixtures, where D_K is the self-diffusion coefficient of K. If the diffusion process of the polymer obeys the reptation model,[19]

$$D_K = D_{1K} N_{eK} N_K^{-2} \quad (6)$$

where D_{1K} and N_{eK} are, respectively, the monomeric diffusion coefficient and the polymerization index between entanglements of K. Equation 5 is called the "slow theory", where the slow component controls the collective diffusion of the system. On the other hand, Kramer et al.,[20] Sillescu,[20] and Brochard[21] proposed the "fast theory". According to this, $\Lambda(0)$ is expressed by

® Abstract published in *Advance ACS Abstracts,* September 1, 1994.

0024-9297/94/2227-6117$04.50/0 © 1994 American Chemical Society

$$\Lambda(0) = \phi_A^2\phi_B^2\left[\frac{D_A N_A}{\phi_A} + \frac{D_B N_B}{\phi_B}\right] \quad (7)$$

and the fast component controls the collective diffusion of the system. Akcasu, Naegele, and Klein[22] calculated $\Lambda(0)$ by using the three-component dynamic random phase approximation approach and proposed the following expression which combines both the slow theory and the fast theory:

$$\Lambda(0) = \phi_A^2\phi_B^2\left[\frac{D_A N_A}{\phi_A} + \frac{D_B N_B}{\phi_B} - \frac{(D_A N_A - D_B N_B)^2}{D_A N_A \phi_A + D_B N_B \phi_B + D_c \phi_c}\right] \quad (8)$$

where D_c and ϕ_c, respectively, are the diffusion coefficient and volume fraction of the vacancy in the mixture. When $D_c\phi_c$ approaches zero and infinity, eq 8 is reduced to eq 5 (the slow theory) and to eq 7 (the fast theory), respectively. This theory was compared with the experimental results.[23]

Schichtel and Binder[12] extended the Chan–Hilliard–Cook theory to a polydisperse A/B polymer blend. According to this theory, if the system is near the spinodal line of the mixture, the time evolutions of $S(q,t)$ and $R(q)$ are given by eqs 1 and 4, respectively, in which $S(q,\infty)$ and $\Lambda(0)$ are modified as follows:

$$\frac{1}{S(q,\infty)} = \frac{1}{\phi_A N_{w,A}} + \frac{1}{\phi_B N_{w,B}} - 2\chi + \frac{1}{18}\left(\frac{N_{z,A}}{N_{w,A}}\frac{a_A^2}{\phi_A} + \frac{N_{z,B}}{N_{w,B}}\frac{a_B^2}{\phi_B}\right)q^2 \quad (9)$$

and

$$\frac{1}{\Lambda(0)} = \frac{\overline{N_A^4}/\overline{N_A^1}}{D_{1,A}N_{e,A}(N_{w,A})^2\phi_A} + \frac{\overline{N_B^4}/\overline{N_B^1}}{D_{1,B}N_{e,B}(N_{w,B})^2\phi_B} \quad (10)$$

for the incompressible systems (the slow theory) where $N_{w,K}$ and $N_{z,K}$ are the weight- and z-average polymerization indices of K, respectively, and the moments $\overline{N_K^m}$ are defined by

$$\overline{N_k^m} = \sum_i x_{N_{i,k}} N_{i,K}^m \quad (11)$$

where $x_{N_{i,k}}$ is the mole fraction of polymer K having polymerization index N_i. It is noted that eq 10 can be reduced to eq 5 by substituting $N_{w,K} = N_{z,K} = \overline{N_K^1} = N_K$ and $\overline{N_K^4} = N_K^4$. It is noted that eq 9 agrees with the static structure factor for the polydisperse mixture obtained by Joanny.[10]

Many experimental results[24-27] support the validity of the linear theory in the early stage of SD. In these studies, however, special attentions were not focused on the MWD effect. Here we aim to critically test the validity of the linearized theory for the mixture with a broad MWD in Section IV, after describing the samples, experimental methods, and the quench depth condition in section II and experimental results in section III. Section V presents the results of the comparison between the experimental results and the theoretical result by Schichtel and Binder.

II. Experimental Section

A. Samples and Sample Preparation. The samples SBR (coded as SBR10) and PB (coded as PB5, PB10, PB20, PB50, and PB100) used in this study were all prepared by using the living anionic polymerization technique with butyllithium as a catalyst and cyclohexane as a solvent. Their characteristic parameters are listed in Table 1 where M_w, M_z, and styrene wt (%) designate the weight-average molecular weight, z-average molecular weight, and weight fraction of styrene monomer in SBR, respectively. M_w and M_z/M_w were measured by GPC-LS. The weight fraction of styrene monomer in SBR10 and the microstructure of the PB part were measured by infrared spectroscopy. The code PBx refers to the PB specimen having M_w close in units of ten thousand.

Table 1. Characterization of Samples Used in This Study

sample	$10^{-4}M_w$	M_z/M_w	styrene wt (%)	microstructure wt (%) 1,4-cis	1,4-trans	1,2-vinyl
SBR10	8.3	1.2	20	17	31	52
PB5	4.9	1.3		23	38	39
PB10	8.9	1.4		24	37	39
PB20	22.3	1.3		23	37	40
PB50	51.9	1.8		24	37	39
PB100	103	2.4		20	29	51

The blend specimens used in this study are listed in Table 2. We prepared two series of the blend specimens. One consists of P5, P10, and P20 of which PB has the different weight-average molecular weight and has a single peak in the MWD. P in Px stands for the blend with SBR10/PBx 50/50 wt %/wt %, while x in Px stands for weight-average molecular weight of PB in the blend. The other is the SBR10/PBx/PBy systems (coded as P5/100, P10/50, and P10/100) to investigate the effects of MWD. Here the numbers x and y in Px/y refer to PBx and PBy, respectively. The SBR10/PBx/PBy system is a mixture of SBR10 and two of PB5, PB10, PB50, and PB100. The PB components in all the SBR10/PBx/PBy blends have different bimodal MWD, but their M_w's are all identical to that of PB20. We made the M_w values of PB identical to make the thermodynamic driving force for SD identical, as will be discussed in section II.C. Therefore the code P5/100 stands for the mixture of SBR10 and PB in which PB is composed of PB5 and PB100 such that the M_w of the mixture PB is equal to that for PB20. In Table 2, $M_{n,PB}$, $M_{w,PB}$, and $M_{z,PB}$, are the number-average, weight-average, and z-average molecular weight of the PB part (i.e., PBx/PBy) in the mixtures, respectively.

B. Experimental Methods. The mixtures listed in Table 2 were dissolved in toluene to prepare homogeneous solutions containing 10 wt % polymer. The solutions were filtered through a Millipore filter with an average pore size of 0.2 μm and then cast into the films of 50 μm thickness in a Petri dish. The solvent was evaporated slowly at 30 °C for 1 week. The films thus obtained were further dried in a vacuum oven at room temperature until their weight became constant.

The as-cast films were opaque because they had phase-separated structures via SD during the solvent evaporation process. Since the critical temperatures for the mixtures are very high, we cannot bring them into a single-phase state by heating. Instead, we brought them into a one-phase state by using the homogenization process induced by Baker's transformation described elsewhere.[26] The 0.1 mm thick homogenized film specimen was sandwiched between thin glass plates and placed in a sample holder, and then the film specimen was heated to 70 °C quickly. The dynamics of phase separation was observed *in situ* by the time-resolved light scattering method described elsewhere.[27] The time right after the homogenization was taken as the origin of time t.

C. Phase Separation Condition. We estimated the parameter $\epsilon_T(T)$ which characterizes the thermodynamic driving force for the phase separation. $\epsilon_T(T)$ is defined by

$$\epsilon_T(T) \equiv [\chi_{eff}(T) - \chi_s]/\chi_s \quad (12)$$

where $\chi_{eff}(T)$ is the effective Flory–Huggins segmental interaction parameter per segment between SBR and PB at the phase separation temperature and χ_s is $\chi_{eff}(T)$ at the spinodal temperature T_s of the mixtures. χ_s is defined by

Table 2. Blend Specimens Used in This Study

code	systems	wt %	$10^{-4}M_{n,PB}$	$10^{-4}M_{w,PB}$	$10^{-4}M_{z,PB}$
P5	SBR10/PB5	50/50	3.5	4.9	6.9
P10	SBR10/PB10	50/50	5.6	8.9	14.2
P20	SBR10/PB20	50/50	17.2	22.3	29.0
P5/100	SBR10/PB5/PB100	50/41.1/8.9	4.18	22.3	204
P10/100	SBR10/PB10/PB100	50/42.9/7.1	6.34	22.3	167
P5/50	SBR10/PB5/PB50	50/31.5/18.5	5.18	22.3	81.5

$$\chi_s \equiv \frac{1}{2}\left(\frac{1}{N_{w,SBR}\phi_{SBR}} + \frac{1}{N_{w,PB}\phi_{PB}}\right) \quad (13)$$

where ϕ_{SBR} and ϕ_{PB} are the volume fractions and $N_{w,PB}$ and $N_{w,SBR}$ are the weight-average polymerization indices of SBR and PB, respectively. In the context of the mean field random phase approximation, $\chi_{eff}(T)$ is approximated by[28]

$$\chi_{eff}(T) \cong (1-\varphi)^2\chi_{SB}(T) \quad (14)$$

where φ is the volume fraction of butadiene units in the SBR chain (φ = 0.803) and $\chi_{SB}(T)$ is the Flory–Huggins segmental interaction parameter between styrene and butadiene. We use for $\chi_{SB}(T)$ the following expression:

$$\chi_{SB}(T) = -0.021 + 25/T \quad (15)$$

which was determined by small-angle X-ray scattering from polystyrene-*block*-polybutadiene.[29]

The values of $\epsilon_T(T)$ calculated with eqs 12–15 are listed in Table 3. The values of $\epsilon_T(T)$ of the Px/y (SBR10/PBx/PBy) system are identical with that of P20 because the $M_{w,PB}$ values of SBR10/PBx/PBy are identical with that of PB20. Except for P5 and P10, the values of $\epsilon_T(T)$ are close to unity. Thus, the phase separation conditions used for the mixtures with $M_{w,PB}$ = 22.3 × 10^4 correspond to a deep quench.

Table 3. Thermodynamic Driving Force

code	$\epsilon_T(T)^a$
P5	0.032
P10	0.40
P20	0.90
P5/100	0.90
P10/100	0.90
P5/50	0.90

[a] Calculated from eqs 12–15.

III. Results

At first, we compare the time changes in the scattered intensity of the three mixtures P5, P10, and P20 whose PB components have different M_w values but have a single-peaked MWD. Figure 1 shows time changes in the light scattering profiles during SD for P5 (a), P10 (b), and P20 (c) at 70 °C. In each figure, the relative scattered intensity of the early stage of SD is plotted as a function of magnitude q of the scattering vector defined by

$$q = \frac{4\pi}{\lambda}\sin\left(\frac{\theta}{2}\right) \quad (16)$$

where λ and θ are the wavelength of the incident beam and the scattering angle in the medium, respectively.

Each part shows the following similar trends: the scattered intensity in the larger q region grows faster than that in the smaller q region, and the peak in the scattered intensity appears at the high q limit covered in this experiment.

Next we shall compare the time changes in the scattered intensity of the four mixtures P20, P5/100, P10/100, and P5/50 whose PB parts have the same M_w's but different MWDs. Figure 2 shows time changes in the time-resolved light scattering profiles for P20 (a), P5/100 (b), P10/100 (c), and P5/50 (d) at 70 °C. These mixtures have the same features as P5 and P10. Moreover, the peaks of the four mixtures at $t \cong 58.5$ min appear at the same $q \cong 8.8 \times 10^{-3}$ nm^{-1}.

IV. Test of Cahn's Linearized Theory in the Early Stage of SD

Figure 3 illustrates the semilogarithmic plot of $I(q,t)$ vs t at various fixed q for (a) P20, (b) P5/100, (c) P10/100, and (d) P5/50. Each part shows the linear relationship between $\ln[I(q,t)]$ and t, indicating that the time evolution

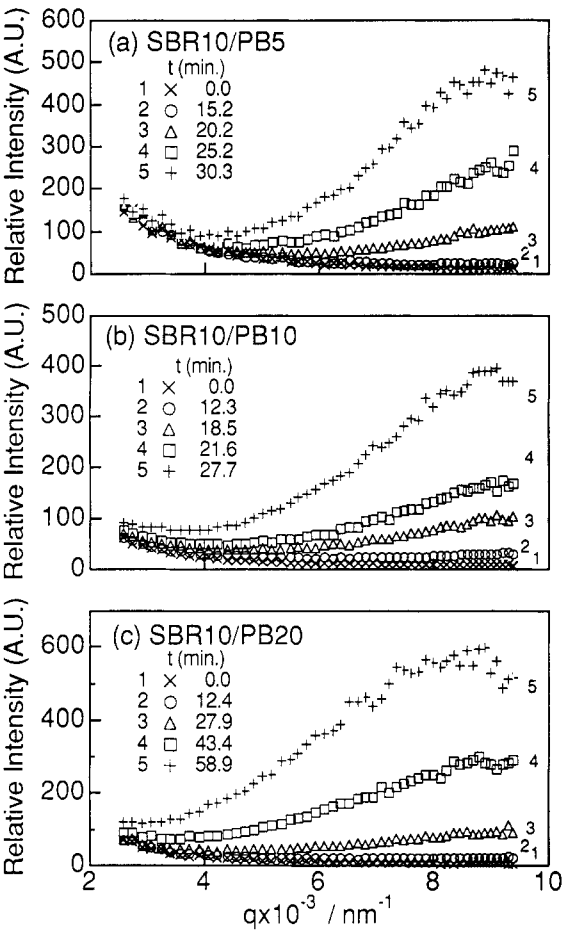

Figure 1. Time changes in the scattered intensity profiles of (a) P5, (b) P10, and (c) P20 after the onset of SD at 70 °C.

of the structure factor obeys Cahn's equation (eq 3) even for the mixtures with bimodal MWDs and that the thermal noise effects are negligible at the time and q domains covered in this experiment. We also found the exponential growth of $I(q,t)$ with t for P5 and P10, though we did not show it here. In previous studies,[30] we found that the homogenization process brings the samples into a single phase near the spinodal point. As pointed out earlier in section II.C, the phase separation condition used in this study corresponds to a deep quench. Therefore the relationship between $S(q,\infty)$ and $S(q,0)$ should satisfy

$$|S(q,\infty)| \ll S(q,0) \quad (17)$$

for the q region covered in this study, so that the thermal

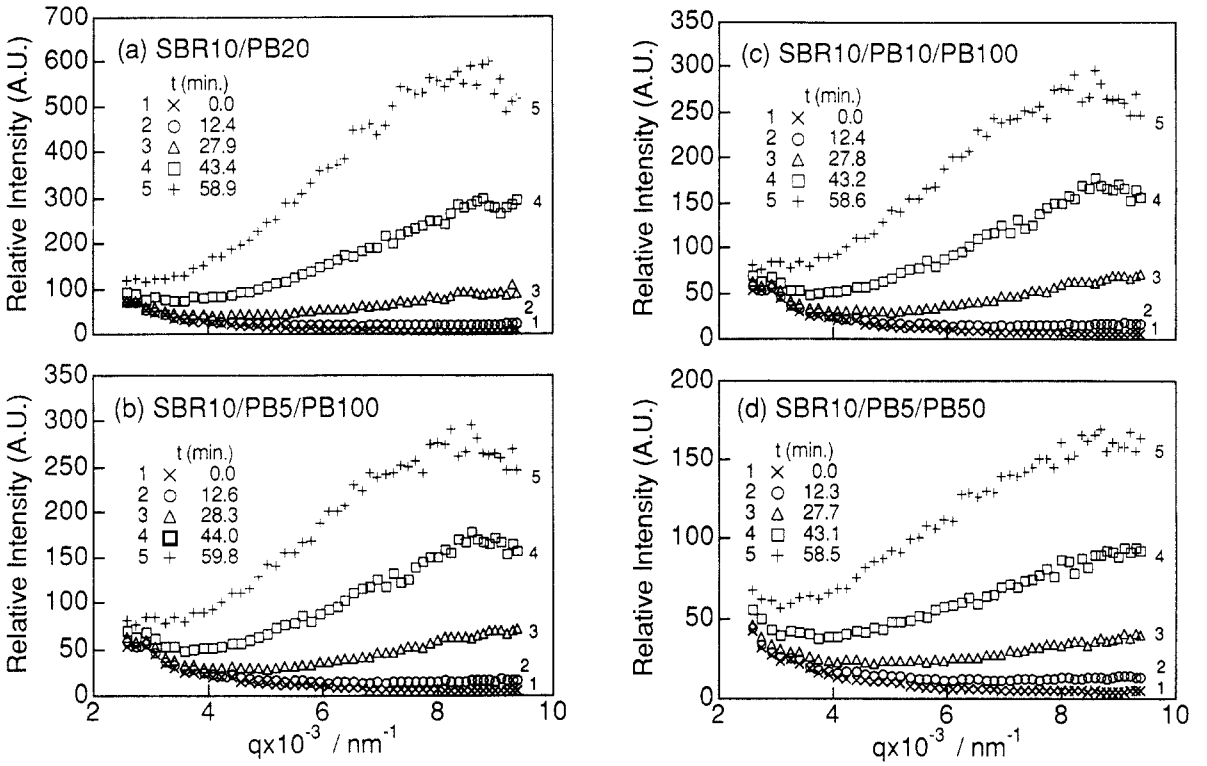

Figure 2. Time changes in the scattered intensity profiles of (a) P20, (b) P5/100, (c) P10/100, and (d) P5/50 after the onset of SD at 70 °C.

noise effects are small, and hence eq 3 is expected to be valid. Deviations from linearity which are observed in the time scale longer than about 35 min are due to the nonlinear effect in the later times of SD.[31]

From the slope of each straight line we can determine $R(q)$ for each mixture. If both components of the mixture are monodisperse, $R(q)$ is given by

$$R(q) = q^2 D_{app}\left[1 - \frac{q^2}{2q_m^2(0)}\right] \tag{18}$$

from eqs 2, 4, and 5 or 7 where D_{app} and $q_m(0)$ are the collective diffusion coefficient and the characteristic wavenumber of the concentration fluctuations in the early stage of SD, respectively. In the case when SBR and PB have no MWD, they are given by[32]

$$D_{app} = \frac{D_{SBR}D_{PB}\bar{N}}{D_{SBR}N_{SBR}\phi_{SBR} + D_{PB}N_{PB}\phi_{PB}}\epsilon_T(T) \quad \text{(slow theory)} \tag{19}$$

or

$$D_{app} = \frac{\bar{N}(D_{SBR}N_{SBR}\phi_{PB} + D_{PB}N_{PB}\phi_{SBR})}{N_{SBR}N_{PB}}\epsilon_T(T) \quad \text{(fast theory)} \tag{20}$$

and

$$q_m^2(0) = \frac{9\bar{N}}{N_{SBR}N_{PB}\overline{a^2}}\epsilon_T(T) \tag{21}$$

where

$$\bar{N} \equiv N_{SBR}\phi_{SBR} + N_{PB}\phi_{PB} \tag{22}$$

and

$$\overline{a^2} \equiv \phi_{SBR}a_{PB}^2 + \phi_{PB}a_{SBR}^2 \tag{23}$$

The corresponding expressions for the mixtures with MWD will be described in section V.

D_{app} and $q_m(0)$ are evaluated from the intercept and slope of the $R(q)/q^2$ vs q^2 plot. Figure 4 shows this plot for the four mixtures with $M_{w,PB} = 22.3 \times 10^4$. Each plot shows the linearity as predicted by eq 18. The exponential growth of $I(q,t)$ and the linear relationship between $R(q)/q^2$ and q^2 suggest that the dynamics of the concentration fluctuations of the early stage SD can be approximated by Cahn's linearized theory even for the mixtures with the bimodal MWD.

V. Parameters Characterizing the Early Stage SD

Table 4 summarizes the characteristic parameters of the early stage SD for the three mixtures with different $M_{w,PB}$ values. Here the characteristic wavelength Λ_m and the characteristic time t_c for the concentration fluctuations of the mixtures in the early stage SD are defined by

$$\Lambda_m \equiv \frac{2\pi}{q_m(0)} \tag{24}$$

and

$$t_c \equiv \frac{1}{D_{app}q_m^2(0)} \tag{25}$$

respectively.

As shown in Table 4, D_{app} decreases with $M_{w,PB}$ but $q_m(0)$ is nearly independent of $M_{w,PB}$. D_{app} depends on $\epsilon_T(T)$ and the diffusion coefficients D_{SBR} and D_{PB} (see eqs 19 and 20). $\epsilon_T(T)$ increases but D_{PB} decreases with $M_{w,PB}$. As discussed in a previous paper,[30] the molecular weight dependence of $\epsilon_T(T)$ is smaller than that of D_{PB}. Hence the molecular weight dependence of D_{app} is dominantly

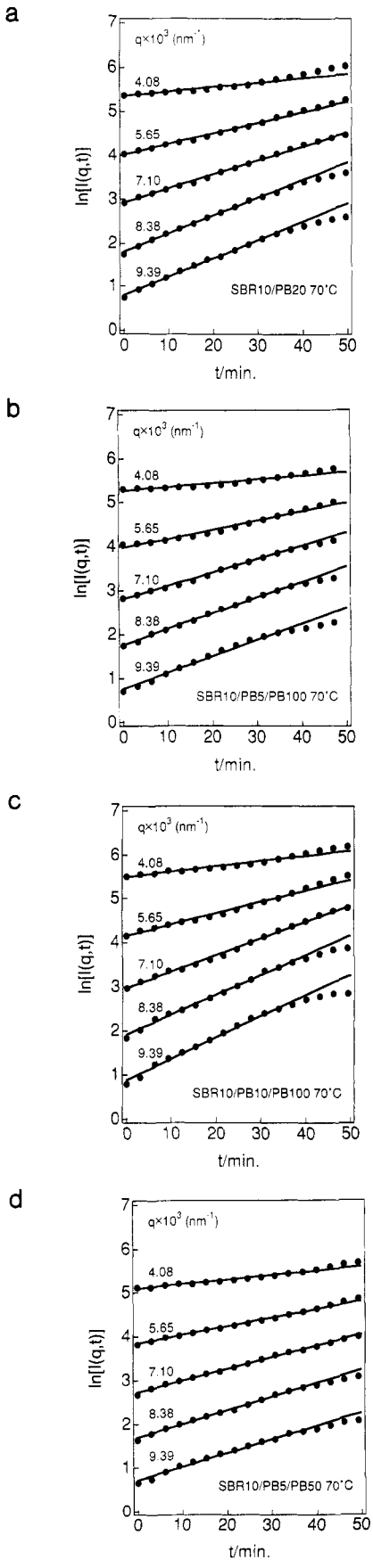

Figure 3. $\ln[I(q,t)]$ vs t at various fixed q for (a) P20, (b) P5/100, (c) P10/100, and (d) P5/50 at 70 °C. Curves are shifted vertically to avoid overlapping: the curve for $q = 9.39 \times 10^{-3}$ nm^{-1} is not shifted but the other curves are shifted up by factor e relative to the neighboring curve.

controlled by that of D_{PB} rather than that of $\epsilon_T(T)$, and as a consequence it decreases with $M_{w,PB}$ as expected.

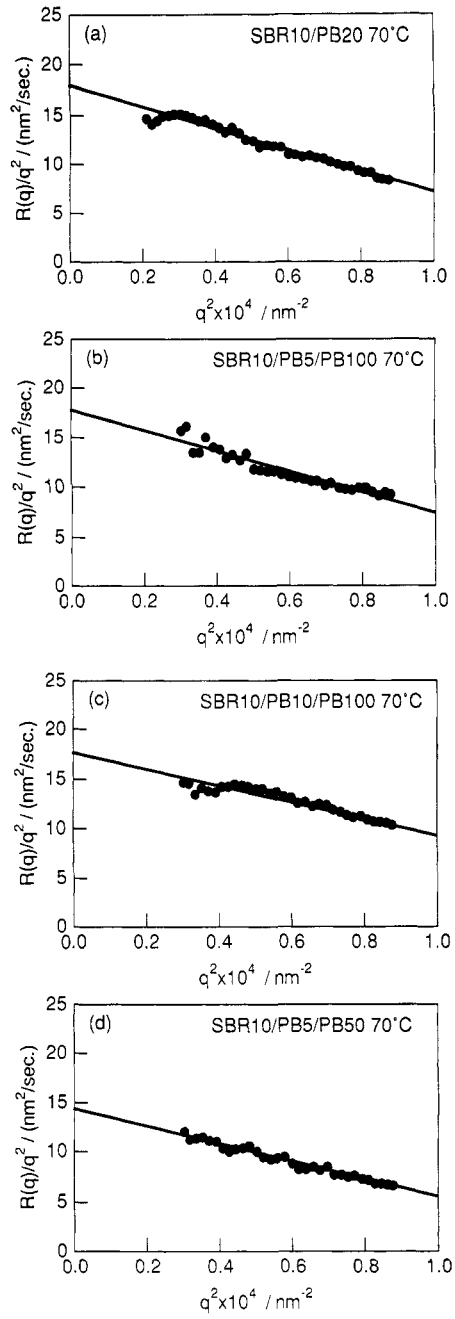

Figure 4. $R(q)/q^2$ plotted as a function of q^2 for (a) P20, (b) P5/100, (c) P10/100, and (d) P5/50 at 70 °C.

Table 4. Characteristic Parameters of Early Stage SD for SBR10/PB$_x$

code	D_{app} (nm^2/s)	$10^3 q_m(0)$ (nm^{-1})	$10^{-2}\Lambda_m$ (nm)	$10^{-2}t_c$ (s)
P5	36.0 ± 2.0	9.0 ± 0.1	7.0 ± 0.1	3.4 ± 0.1
P10	26.4 ± 0.6	10.2 ± 0.1	6.2 ± 0.1	3.6 ± 0.1
P20	17.9 ± 0.6	9.1 ± 0.2	6.9 ± 0.1	6.7 ± 0.1

$q_m(0)$ consists of the $\epsilon_T(T)$ part and the front part $[9\bar{N}/(N_{SBR}N_{PB}a^2)]$ (see eq 21). The front part decreases with $M_{w,PB}$ but $\epsilon_T(T)$ increases with $M_{w,PB}$. The molecular weight dependence of $\epsilon_T(T)$ and that of the front term may be canceled out so that $q_m(0)$ is expected to be insensitive to $M_{w,PB}$.

Table 5 shows the characteristic parameters of the early stage SD for the four mixtures with the fixed $M_{w,PB} = 22.3 \times 10^4$. It indicates that D_{app} and $q_m(0)$ (and other parameters) are insensitive to MWD, as long as the $M_{w,PB}$ values are identical. The growth rate $R(q)$ even for the mixture with a broad MWD could be assumed to consist

Table 5. Characteristic Parameters of Early Stage SD for SBR10/PB$_x$/PB$_y$

code	D_{app} (nm^2/s)	$10^3 q_m(0)$ (nm^{-1})	$10^{-2}\Lambda_m$ (nm)	$10^{-2}t_c$ (s)
P20	17.9 ± 0.6	9.1 ± 0.2	6.9 ± 0.1	6.7 ± 0.1
P5/100	17.8 ± 0.7	9.2 ± 0.3	6.7 ± 0.1	6.6 ± 0.2
P10/100	17.6 ± 1.0	10.2 ± 0.5	6.2 ± 0.3	5.4 ± 0.3
P5/50	14.3 ± 0.5	9.0 ± 0.2	7.0 ± 0.1	8.6 ± 0.2

of the dynamical part $\Lambda(0)$ and thermodynamic part $1/S(q,\infty)$ (see eq 4). The self-diffusion coefficient[33] depends on N_w so that $\Lambda(0)$ is expressed by

$$\frac{1}{\Lambda(0)} = \frac{1}{D_A\sum_i N_{A,i}\phi_{A,i}} + \frac{1}{D_B\sum_i N_{B,i}\phi_{B,i}} = \frac{1}{D_{1A}N_{eA}N_{w,A}^{-1}\phi_A} + \frac{1}{D_{1B}N_{eB}N_{w,B}^{-1}\phi_B} \quad (26)$$

in the context of the slow theory, or

$$\Lambda(0) = D_A\phi_B^2\sum_i N_{A,i}\phi_{A,i} + D_B\phi_A^2\sum_i N_{B,i}\phi_{B,i} = D_{1A}N_{eA}N_{w,A}^{-1}\phi_A\phi_B^2 + D_{1B}N_{eB}N_{w,B}^{-1}\phi_B\phi_A^2 \quad (27)$$

in the context of the fast theory. $S(q=0,\infty)$ also depends on N_w:

$$\frac{1}{S(0,\infty)} = \frac{1}{\phi_A N_{w,A}} + \frac{1}{\phi_B N_{w,B}} - 2\chi \quad (28)$$

The products of $\Lambda(0)$ and $1/S(q=0,\infty)$ or D_{app}, hence, depend on M_w. In this case the results obtained in Table 5 seem to be reasonable.

Finally, we test the Schichtel and Binder theory.[12] The theory gives the following characteristic parameters in the context of the slow theory:

$$D_{app} = \{[D_{1A}N_{eA}D_{1B}N_{eB}N_{w,A}N_{w,B}(\overline{N_{w,A}\phi_A} + \overline{N_{w,B}\phi_B})]/[D_{1B}N_{eB}(N_{w,B})^2\phi_B(\overline{N_A^4}/\overline{N_A^1}) + D_{1A}N_{eA}(N_{w,A})^2\phi_A(\overline{N_B^4}/\overline{N_B^1})]\}\epsilon_T(T) \quad (29)$$

and

$$q_m^2(0) = \frac{9\left(\frac{1}{N_{w,A}\phi_A} + \frac{1}{N_{w,B}\phi_B}\right)}{\left(\frac{N_{z,A}a_A^2}{N_{w,A}\phi_A} + \frac{N_{z,B}a_B^2}{N_{w,B}\phi_B}\right)}\epsilon_T(T) \quad (30)$$

where A and B correspond to SBR and PB, respectively. In eq 29 D_{app} is divided into two parts: the thermodynamic part $\epsilon_T(T)$ and the transport part (the part in parenthesis in eq 29). $\epsilon_T(T)$ depends only on M_w so that the effects of the MWD on D_{app} for the four mixtures with the same M_w depend on the transport term, i.e., the moments of polymerization index and monomeric diffusion coefficients. Equation 29 is rewritten as follows:

$$D_{app} = D_{1A}N_{eA}\epsilon_T(T) \times \left[\frac{\alpha N_{w,A}N_{w,B}(\overline{N_{w,A}\phi_A} + \overline{N_{w,B}\phi_B})}{\alpha(N_{w,B})^2\phi_B(\overline{N_A^4}/\overline{N_A^1}) + (N_{w,A})^2\phi_A(\overline{N_B^4}/\overline{N_B^1})}\right] \quad (31)$$

$$\equiv D_{1A}N_{eA}\epsilon_T(T)\psi \quad (32)$$

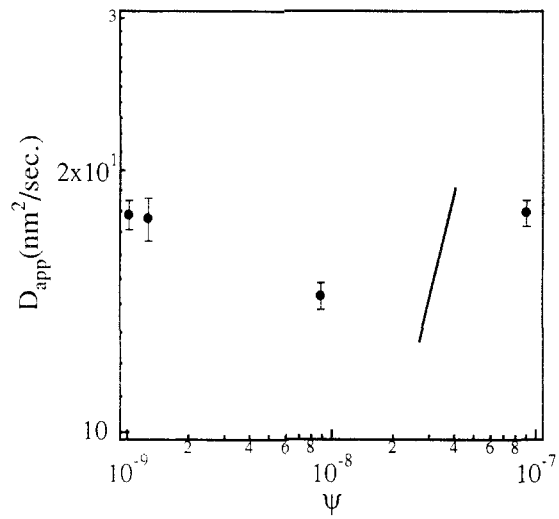

Figure 5. D_{app} plotted as a function of ψ. ψ is defined in eq 32. The solid line has a slope of 1.

where we define the quantity ψ by the quantity in parenthesis in the right hand side of eq 31, and α is defined by

$$\alpha \equiv D_{1B}N_{eB}/D_{1A}N_{eA} \quad (33)$$

In Figure 5, D_{app} is plotted as a function of ψ. Here we assume that $\alpha = 1$, as used in a previous paper.[32] If the data obey the theory, the slope of the plot should be 1, as illustrated by the straight line in Figure 5. However the experimental results do not support the theory. The possible reasons of the failure may be that the quench depth we used in this experiment is a deep quench though the theory dealing with the MWD is valid near the spinodal point.

VI. Concluding Remark

In the present paper, the time changes in the scattered intensity profiles for the SBR/PB blends with PB having different MWDs were investigated by the time-resolved light scattering technique. The early stage SD of the mixtures was well described by Cahn's linearized theory, as in the case of the mixtures having relatively narrow MWDs. The characteristic parameters thus determined for the early stage SD were found to be insensitive to MWD but to be sensitive to M_w. The Schichtel and Binder theory failed to explain our experimental results probably because the quench depth we used was deep. The theory would be expected to describe the dynamics of the early stage SD for polydisperse binary mixtures at shallow quench conditions. Hence experiments at shallow quench conditions are needed for comparison with the theory and a theory is also needed to explain our experimental results.

Acknowledgment. We are greatly indebted to Japan Synthetic Rubber Co. Ltd. for supplies of SBR and PB samples.

References and Notes

(1) Gunton, J. D.; San Miguel, M.; Sahni, P. In *Phase Transition and Critical Phenomena*; Domb, C., Lebowitz, J. L. Eds.; Academic Press: New York, 1983; p 269.
(2) Binnder, K. In *Phase Transformation in Materials*; Haasen, D., Ed. Nol.); Materials Science and Technology; Cahn, P. H. R. W., Haasen, P., Kramer, E. J., Eds.; VCH: Weinheim, 1991; Vol. 5, Chapter 7, pp 405.
(3) Hashimoto, T. *Phase Transitions* **1988**, *12*, 47. Hashimoto, T. In *Structure and Properties of Polymers*; Thomas, E. L., Ed.

(Vol.); Materials Science and Technology; Cahn, P. H. R. W., Haasen, P., Kramer, E. J., Eds., VCH: Weinheim, 1993; Vol. 12, p 254.
(4) Oono, Y.; Puri, S. *Phys. Rev. A.* **1988**, *38*, 434. Puri, S.; Oono, Y. *Phys. Rev. A* **1988**, *38*, 1542. Toral, R.; Chakrabarti, A.; Gunton, J. D. *Phys. Rev. Lett.* **1988**, *60*, 2311. Chakrabarti, A.; Toral, A.; Gunton, J. D.; Muthukumar, M. *Phys. Rev. Lett.* **1989**, *63*, 2072. Chakrabarti, A.; Toral, A.; Gunton, J. D.; Muthukumar, M. *J. Chem. Phys.* **1990**, *92*, 6899.
(5) Shinozaki, A.; Oono, Y. *Phys. Rev. Lett.* **1991**, *66*, 173.
(6) Koga, T.; Kawasaki, K. *Phys. Rev. A* **1991**, *44*, R817.
(7) Koga, T.; Kawasaki, K.; Takenaka, M.; Hashimoto, T. *Physica A* **1993**, *198*, 473.
(8) Shinozaki, A.; Oono, Y. *Phys. Rev. E.* **1993**, *48*, 2622.
(9) Hashimoto, T.; Takenaka, M.; Jinnai, H. *J. Appl. Crystallogr.* **1991**, *24*, 457. Takenaka, M.; Hashimoto, T. *J. Chem. Phys.* **1992**, *96*, 6177.
(10) Joanny, J. F. *C. R. Seances Acad. Sci., Ser. B* **1978**, *286*, 89.
(11) Koningsveld, R.; Staverman, A. J. *J. Polym. Sci.* **1968**, *A26*, 305.
(12) Schichtel, T. E.; Binder, K. *Macromolecules* **1987**, *20*, 1671.
(13) Takenaka, M.; Hashimoto, T. *Phys. Rev. E* **1993**, *48*, R647.
(14) Cahn, J. W. *J. Chem. Phys.* **1965**, *42*, 93.
(15) Cook, H. E. *Acta Metall.* **1970**, *18*, 297.
(16) de Gennes, P. G. *J. Chem. Phys.* **1980**, *72*, 4756.
(17) Pincus, P. *J. Chem. Phys.* **1981**, *75*, 1996.
(18) Binder, K. *J. Chem. Phys.* **1983**, *79*, 6387.
(19) Doi, M.; Edwards, S. F. *The theory of Polymer Dynamics*; Clarendon Press: London, 1986.
(20) Kramer, E. J.; Green, P.; Palmstrom, C. J. *Polymer* **1984**, *25*, 473. Sillescu, H. *Makromol. Chem., Rapid Commun.* **1984**, *5*, 519.
(21) Brochard, F. In *Molecular Conformation and Dynamics of Macromolecules in Condensed Systems*; Nagasawa, M., Ed.; Elsevier: New York, 1988; p 249.
(22) Akcasu, A. Z.; Naegele, G.; Klein, R. *Macromolecules* **1991**, *24*, 4408.
(23) Feng, Yi.; Han, C. C.; Takenaka, M.; Hashimoto, T. *Polymer* **1989**, *33*, 2729.
(24) Snyder, H. L.; Meakin, P.; Reich, S. *Macromolecules* **1983**, *16*, 757. Izumitani, T.; Hashimoto, T. *J. Chem. Phys.* **1985**, *83*, 3694. Hashimoto, T.; Itakura, M.; Masegawa, H. *J. Chem. Phys.* **1986**, *85*, 6118. Kumaki, J.; Hashimoto, T. *Macromolecules* **1986**, *19*, 763. Kyu, T.; Saldanha, J. M. *Macromolecules* **1988**, *21*, 1021.
(25) Okada, M.; Han, C. C. *J. Chem. Phys.* **1986**, *85*, 5317. Sato, T.; Han, C. C. *J. Chem. Phys.* **1988**, *88*, 2057.
(26) Hashimoto, T.; Izumitani, T.; Takenaka, M. *Macromolecules* **1989**, *22*, 2293.
(27) Hashimoto, T.; Kumaki, J.; Kawai, H. *Macromolecules* **1983**, *16*, 641.
(28) Mori, K.; Tanaka, H.; Hashimoto, T. *Macromolecules* **1987**, *20*, 381.
(29) Owens, J. N.; Gancarz, I. S.; Koberstein, J. T.; Russel, T. P. *Macromolecules* **1989**, *22*, 3380.
(30) Hashimoto, T.; Izumitani, T.; Takenaka, M. *Macromolecules* **1989**, *19*, 2293.
(31) Langer, J. S.; Bar-on, M.; Miller, H. D. *Phys. Rev. A* **1975**, *11*, 1417.
(32) Takenaka, M.; Izumitani, T.; Hashimoto, T. *Macromolecules* **1987**, *20*, 2257.
(33) Graessley, W. J. *Polym. Sci., Polym. Phys. Ed.* **1980**, *18*, 27.